 doi:10.20944/preprints202010.0111.v1

Article

Optimizing Window Design on Residential Building Facades by Considering Heat Transfer and Natural Lighting in Non-tropical Regions of Australia

Zixuan Chen [1], Ahmed W A Hammad [1,*], Imriyas Kamardeen [2] and Assed Haddad [3]

[1] UNSW Built Environment, Construction Management Discipline, UNSW Sydney, Australia
[2] School of Architecture & Built Environment, Deakin University, Australia
[3] Escola Politécnica / Departamento de Construção Civil, Universidade Federal do Rio de Janeiro, Brazil
* Correspondence: a.hammad@unsw.edu.au

Abstract: Windows account for a significant proportion of the total energy lost in buildings. The interaction of window type, Window-to-Wall Ratio (WWR) scheduled and window placement height would influence the natural lighting and heat transfer through windows. This is a pressing issue for non-tropical regions considering their high emissions and distinct climatic characteristics. A limitation exists in the adoption of common simulation-based optimisation approaches in the literature, which are hardly accessible to practitioners. This article develops a numerical-based window design optimisation model using a common Building Information Modelling (BIM) platform adopted throughout the industry, focusing on non-tropical regions of Australia. Three objective functions are proposed; the first objective is to maximize the available daylight, and the other two emphasize on the undesirable heat transfer through windows in summer and winter respectively. The developed model is tested on a case study located in Sydney, Australia, and a set of Pareto-optimum solutions is obtained. Through the use of the proposed model, energy savings of up to 16.43% are achieved. Key findings on the case example indicate that leveraging winter heat gain to reduce annual energy consumption should not be the top priority when designing windows for Sydney.

Keywords: Multi-objective; Optimisation; Revit; Dynamo; BIM; Window design; Window type; Window position; Window-to-Wall Ratio

Table 1 - Nomenclature

ABBREVIATIONS	
BIM	Building Information Modelling
CSV	Comma-separated Value file format
GBI	Green Building Initiative
HVAC	Heating, ventilation, and air conditioning
IFC	Industry Foundation Classes
MOO	Multi-objective Optimisation
NCC	National Construction Code
NSGA-II	Non-Dominated Sorting Genetic Algorithm
SHGC	Solar Heat Gain Coefficient
VLT	Visual Light Transmittance

Preprints (www.preprints.org) | NOT PEER-REVIEWED | Posted: 6 October 2020 doi:10.20944/preprints202010.0111.v1

VPL	Visual Programming Language
U	Conduction Coefficient
WFR	Window-to-Floor Ratio
WWR	Window-to-Wall Ratio
SET	
$\boldsymbol{i} \in \{\mathbf{1} \dots \boldsymbol{n}\}$, $\boldsymbol{i} \in \boldsymbol{N}$	Set of walls with windows scheduled on each story
OBJECTIVE FUNCTIONS	
$\boldsymbol{EA}$	*Effective Aperture* calculated on each floor.
$\boldsymbol{HG'}$	A general function for calculating overall heat gain.
$\boldsymbol{HL'}$	A general function for calculating overall heat loss.
$\boldsymbol{HL}$	*Winter Heat Loss* calculated on each floor.
$\boldsymbol{HG}$	*Summer Heat Gain* calculated on each floor.
VARIABLES	
$\boldsymbol{VLT}$	Visual Light Transmittance for the window system
$\boldsymbol{SHGC}$	Solar Heat Gain Coefficient for the window system
$\boldsymbol{U}$	Conduction Coefficient for the window system
$\boldsymbol{WWR_i}$	WWR scheduled for the wall i
$\boldsymbol{ES_i}$	*Summer Exposure Factor* of the wall i.
$\boldsymbol{EW_i}$	*Winter Exposure Factor* of the wall i.
$\boldsymbol{\delta_g}$	Binary variable which is equal to 1 when *Summer Heat Gain* exceeds the maximum value allowed, and 0 otherwise.
$\boldsymbol{\delta_l}$	Binary variable which is equal to 1 when *Winter Heat Loss* exceeds the maximum value allowed, and 0 otherwise.
$\boldsymbol{\delta_h}$	Binary variable which is equal to one when the Window Placement Constraint is violated, and 0 otherwise.
$\boldsymbol{\delta_f}$	Binary variable which is equal to one when the Window-to-Floor Ratio Constraint is violated, and 0 otherwise.
PARAMETERS	
$\boldsymbol{WA}$	Total window area on each story.
$\boldsymbol{I}$	Solar irradiance.
$\boldsymbol{p}$	The width of the shading device.
$\boldsymbol{h}$	The distance between the base of the window to the bottom of the shading device.
$\boldsymbol{A_i}$	Gross area of the hosting wall i.
$\boldsymbol{H_i}$	Height of the hosting wall i.
$\boldsymbol{WP}$	A hypothetical working plane determined by the designer.
$\underline{\boldsymbol{WH_i}}$	Lower bound for window placement on the wall i.
$\overline{\boldsymbol{WH_i}}$	Upper bound for window placement on the wall i.
$\underline{\boldsymbol{WFR}}$	The minimum WFR specified by the designer.
$\overline{\boldsymbol{WFR}}$	The maximum WFR specified by the designer.
$\boldsymbol{F}$	The fully enclosed covered area on each floor.

Preprints (www.preprints.org) | NOT PEER-REVIEWED | Posted: 6 October 2020 doi:10.20944/preprints202010.0111.v1

$\overline{HG}$	Maximum value allowed for *Summer Heat Gain*.
C_{SHGC}	Deemed-to-satisfy constant for calculating *Summer Heat Gain* obtained from the National Construction Code (NCC)
$\overline{CON}$	Maximum value allowed for *Winter Heat Loss*
C_U	Deemed-to-satisfy constant for calculating *Winter Heat Loss* obtained from the National Construction Code (NCC)
P	Constant penalty
PENALTY FUNCTIONS	
$f_{p1}(HG)$	Penalty function applied to the design objective *Summer Heat Gain*.
$f_{p2}(HL)$	Penalty function applied to the design objective *Winter Heat Loss*.
$f_{p3}(EA)$	Penalty function applied to the design objective *Effective Aperture*.

1. Introduction

The built environment accounts for up to 40 percent of the global energy consumption. Greenhouse gas emission is anticipated to double by 2030 if no actions are taken [84]. Among all sectors in the built environment, residential buildings on average contribute to around three quarters of the total energy consumption [85]. Building performance varies notably across countries and regions. With this in mind, there needs to be alternative measures adopted to enhance the sustainability of buildings based on the local climate of the region in which they are built. Building design offers a great opportunity to address energy consumption involved. This includes numerous passive measures which are incorporated into design strategies to reduce energy consumption [19]. Passive design features can achieve more than 50% reduction in energy expenditure [28]. In particular, the glazing system, regarded as an important design consideration, is responsible for approximately 47% of total energy loss from the residential building envelope; this is attributed to the comparatively high thermal conductivity values of windows [23], which can lead to more extensive use of mechanical heating and cooling. A study found that US residential windows contribute to 32 percent of the total building heating ventilation and air conditioning (HVAC) load [7]. By nature, windows have weak thermal effects, causing undesirable heat loss in cold climates and heat gain in warmer regions [38]. Studying the impact that windows have on energy loss requires an understanding of associated intrinsic optical properties [75], including Visual Light Transmittance (VLT), Solar Heat Gain Coefficient (SHGC), and Conduction Coefficient (U value). One square meter of double-glazing window can lose more than ten times as much heat as the same area of a properly insulated wall [44]. Gong et al. [33] investigated passive design strategies by altering window sizes in different climate zones in China and found that thermal load doubled after increasing Window-to-Wall Ratio (WWR) from 0.15 to 0.6 in cooling-dominated climate. That said, smaller window areas could limit the natural daylight penetration to the interior, leading to the use of artificial lights in order to fulfil lighting requirements [61]. This can be partially compensated by positioning windows at suitable height to allow for a deeper solar penetration [17, 60].

Glazing type is reported as one of the most influential passive window design factors [52]. Arasteh [6] reviewed the advancement of glazing technology, focusing on modifications done in terms of glass properties for thermal and lighting purposes. Cheung et al. [22] studied glazing types' influence on a passive envelope design in hot and humid climates and reported a 4.6% reduction in annual cooling load by applying reflective coating on glazing. In terms of window positioning, Bokel [17] investigated impacts of window placement height on the heating and cooling energy. Further to

this, Kim et al.[41] reported a 1% reduction on total thermal load by placing windows at middle height.

Choosing an appropriate window design is a challenging task. On the one hand, increasing the size of windows will lead to an increase in the amount of daylight [30,50]. At the same time, this will inevitably increase the amount of energy lost through the window [33]. As such, window properties, size and position are three highly interrelated parameters that would affect available natural daylight and heat transfer through windows [54]. The window design dilemma is extremely challenging for non-tropical regions given that these areas account for more emissions and carbon footprint, in comparison to tropical nations [89], and their distinct seasonal meteorology characteristics [78] call for more diverse thermal and lighting design requirements.

To deal with window design problems, the state-of-the-art method discussed in the literature is based on a simulation-based approach [59]. However, several limitations of this approach have been identified, including the need for sophisticated training and expertise to conduct the simulations, time-consuming nature of the method, and its ill-adapted nature [11]. Given the time and resource constraints, along with the limited training of design and construction practitioners in these fields [10], there is a need for developing an easy-to-handle tool that caters for common building modelling software that is utilized in the field.

This paper proposes a novel approach which automatically optimizes window designs, including the window type, which extends the notion of glazing type to include the framing materials, and the WWR, and window placement height, as a response to the current limitation in the literature. The aim of this research is to investigate the feasibility of conducting a numerical-based optimisation in a user-friendly modelling environment, focusing on the three design criteria mentioned above to enhance energy and daylighting aspects in non-tropical regions of Australia. The objective is to deliver an optimisation tool using a common BIM platform utilized in industry (Revit) [15] and to test the proposed approach on a case study.

This paper is structured as follows. A literature review is presented in the next section to help identify methodological limitations in the current knowledgebase and to give an overview of the thermal and lighting mechanism of windows. Following that the research methodology and process are discussed in which an optimisation framework is proposed in Revit and Dynamo [14], a Revit extension, to maximize the available daylight and minimize undesirable heat transfer, while considering the type of window, and its size and placement height. The next section presents a case study with the optimum design solutions visualized. Finally, concluding remarks on passive window design strategies are offered.

2. Literature Review

2.1. Optimisation Technique

In the literature, sustainable design optimisation can be classified as either simulation-based optimisation or numerical-based optimisation [59]. Simulation-based optimisation searches for the optimum design criteria based on the outcomes of a simulation [10]. Although there are several commercial optimisation software available, it is reported that they are time-consuming, and not user-friendly [11]; such approaches do not seem to fit well in real-life design procedures. To fill in this gap, modelling software, such as Rhino [72] and Revit are both incorporated with optimisation packages. Popular packages include Octopus [62], Galapagos [29] and Optimo [69]. Both Octopus and Galapagos are available for Grasshopper [71], a visual programming platform exclusively designed for Rhino [39]. Optimo is a plugin for Dynamo, a visual programming tool used in Revit, and is interoperable with other BIM-based services [40, 76].

These software can deliver a simulation-based optimisation workflow that updates the target model with the desirable design parameters seamlessly [21, 83]. A few attempts have been made to formulate different window design problems using optimisation packages in modelling environment. Table 2 summarizes some key features presented in the studies and the optimisation software employed. It can be concluded that the majority of previous works was carried out in

 doi:10.20944/preprints202010.0111.v1

Rhino/Grasshopper environment with Honeybee and Ladybug packages as the energy simulation engines, which are powered by *Radiance* [46], *EnergyPlus* programs [64] and DOE-2 [36]. As a result, previous research studies have demonstrated the possibility of building optimisation workflows using either Rhino/Grasshopper or Revit/Dynamo. Note that the energy and daylight simulation packages in Dynamo are customized [70] and are not available to the public. The challenge is further exacerbated due to the fact that Dynamo is reported to have occasional compatibility issues with other energy simulation plugins due to the dependency of such plugins on Dynamo build; this is inevitable given that the plugins are mostly contributed and maintained by third party developers [82]. Despite these limitations, if Dynamo is adopted for a numerical-based optimisation problem, there would be minimum dependencies on external packages. This can help alleviate the problem and hence can lead to a more efficient workflow given Revit/Dynamo are integrated with other BIM services [39, 70].

Table 2 - Relevant Studies Presented in the Literature

Reference	Factor(s) Studied	Objective(s)	Method	Optimisation Software	Simulation Tool(s)
[70]	-Window dimensions - Glazing type	LEED Illuminance Level & Annual Energy Cost	Simulation-based	Dynamo+ Optimo	Energy & Daylight Simulation Package
[68]	- Window areas	Useful Daylight Illuminance	Simulation-based	Grasshopper+ Galapagos	Honeybee & Ladybug
[68]	- Window areas	Thermal Energy Consumption	Simulation-based	Grasshopper+ Galapagos	Honeybee & Ladybug
[21]	-Wall thermal properties -Glazing properties -Window dimensions - Façade orientation	Daylight Factor & Normalized Thermal Factor	Simulation-based & Numerical-based	Dynamo+ Optimo	Honeybee
[27]	-South and north-facing window width -Skylight orientation -Skylight dimensions -Skylight location - Louvre length	Useful Daylight Illuminance & Energy Use Intensity	Simulation-based	Grasshopper+ Octopus	Honeybee & Ladybug

	- Building depth -Roof ridge location					
[77]	- WWR - Window height -Number of windows - Sill height	Useful Daylight Illuminance & Energy Use Intensity	Simulation-based	Grasshopper+ Octopus	Honeybee & Ladybug	

2.2. Window Lighting and Thermal Effects

In an early work that examined the influence of glazing on buildings' lighting requirements and energy usage, the term *Effective Aperture* was defined as the product of WWR and VLT [37]. The same study also found that there was a negative relationship between the *Effective Aperture* and the lighting energy consumption. However, as *Effective Aperture* increases, the lighting energy saving starts to level off because of constraints such as latitude and solar radiation to the site [47]. In a subsequent study, the term *Solar Aperture*, obtained by multiplying the SHGC by WWR [48], was introduced to capture the effect of solar heat gain and was coupled with *Effective Aperture* to predict the cooling and lighting energy consumption in warm regions [79]. Sullivan et al. [79] found that once the 'saturation level' is reached, cooling load continues to increase due to solar heat gain, and further electricity savings can only be realized via leveraging *Solar Aperture*. Although the authors acknowledged *Effective Aperture* and *Solar Aperture* alone are not adequate to predict the energy consumption without modelling the effects of heat loss [79], the term *Effective Aperture* nowadays is often used as an indicator of daylight availability in the interior of building spaces [25, 73].

Heat gain through windows occurs when solar radiation enters the interior, or as the result of the conduction of heat absorbed through the window [74]. However, for non-tropical regions solar radiation is the most prominent source of heat gain [19,54], while conduction contributes more to heat loss in winter times [54].

As evidenced by the literature above, there is a lack of method that is readily available and can be easily integrated into BIM procedures. The next section will present a novel framework for automatically designing the WWR, window type and window placement height and the formulation of these design criteria. As a result, minimizing undesirable *Summer Heat Gain* and *Winter Heat Loss*, while maximizing *Effective Aperture* are the objectives of the window design optimisation problem examined herein. It is critical to clarify that the detailed geometry of windows on each façade is not the focus of the study. In fact, Acosta et al. [1] had demonstrated that window shape has no effect on the energy consumption of a building.

3. Methodology

3.1. Optimisation Framework

Fig. 1 summarises the window optimisation framework proposed in the developed approach. Optimo is a Multi-objective Optimisation (MOO) plugin that is readily downloadable as a package in Dynamo. It employs Non-Dominated Sorting Genetic Algorithm (NSGA-II), which is a Multi-objective Evolutionary Algorithm that uses nondominated sorting [24]. NSGA-II is one of the most commonly used algorithms in dealing with multi-objective building design problems [26]. The accuracy of Optimo has been validated by Rahmani Asl et al. [69] and it was proven to be a robust NSGA-II optimisation tool. The building needs not be designed in a particular BIM software so long as it is in the Industry Foundation Classes (IFC) file format. Stage 1 of the framework involves defining three classes of optimisation input, namely:(i) optimisation variables and parameters; (ii) population size and iteration number; and (iii) fitness functions. To define the optimisation variables and parameters, Visual Programming Language (VPL) is used to interact with Revit and extract user

Preprints (www.preprints.org) | NOT PEER-REVIEWED | Posted: 6 October 2020 doi:10.20944/preprints202010.0111.v1

defined geometries from the building model. Available design options can be listed down and then retrieved from a separate Comma-Separated Values (CSV) files. Optimo requires user inputs to specify acceptable ranges for the variables optimised.

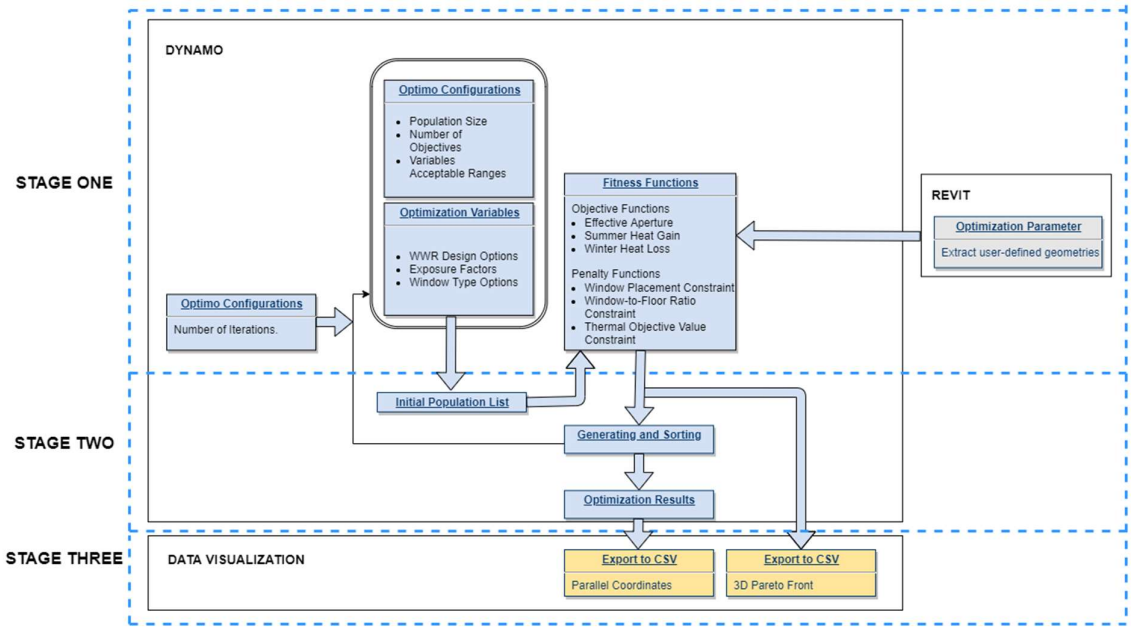

Figure 1 - Proposed Optimisation Framework

The population size, that is defined as the total number of random values needs to be specified as it will be used as the input for the next generation in NSGA-II. The user will also specify a targeted iteration that would terminate the optimisation process. *Fitness Functions* in Optimo context refer to customised functions that evaluate the design objectives [70]. In this study three design objectives as discussed earlier are constructed, namely maximising *Effective Aperture*, minimising *Summer Heat Gain* and minimising *Winter Heat Loss*; all the objectives are formulated as part of the *Fitness Functions* in a Dynamo interpretable format using VPL, DesignScript [2] and Python.

Penalty functions are also included in *Fitness Functions* to penalize values that do not satisfy three classes of constraints identified from the optimisation model. The first type of constraint is related to the architectural model. It defines the model boundaries for window placement. The second type specifies a Window-to-Floor Ratio (WFR) range to prevent overglazing. The third constraint draws upon the nationwide construction regulation in Australia, the National Construction Code (NCC) [56], which states a maximum value allowed for the heat transfer through windows.

At Stage 2 (**Fig. 1**), a list of random values for the variables to be optimized is created as the initial generation for the Optimisation. This will be used as the input for the customized *Fitness Functions*, from which the results are to be evaluated using the NSGA-II algorithm. This process is iterative and only stops when it reaches the pre-determined number of iterations. NSGA-II generates a spread of equally optimal solutions such that any variable cannot be further improved without compromising at least one other variable, which is commonly known as Pareto Front. Note that during this process, *Fitness Function* results at each generation and points on the Pareto Front are both to be exported and saved in a CSV file for further visual analysis in Stage 3.

At the final stage, Stage 3, the exported datapoints will be visualized for subsequent analysis. Design criteria and corresponding objective values at each generation are to be displayed in a 3-dimensional scatter plot to show improvements as the iteration proceeds. A sample of points selected

Preprints (www.preprints.org) | NOT PEER-REVIEWED | Posted: 6 October 2020 doi:10.20944/preprints202010.0111.v1

from the final Pareto Front is plotted using parallel coordinates to visualize the highly interrelated design parameters.

A number of assumptions are made for the framework presented above, based on existing design practices in industry:

- On each story level, windows facing the same direction should be placed at the same height.
- The overall window system is installed with the same type of window.
- Shading devices attached on the same wall face have the same width, measured as

the perpendicular distance from the edge of the shading device to the wall [54].

From here on, window elements discussed in this paper refer to windows located on the building envelope and their framing system.

3.2. Computing Effective Aperture

E*ffective Aperture* in this study is used as a measure to assess the daylight availability, with a larger value indicating less reliance on artificial lights [49], contributing to potential savings in energy consumption. Since no skylights are discussed in this paper, the equation of '*effective aperture for vertical fenestration*' offered by Green Building Initiative (GBI) in ANSI/GBI 01-2019 [5] is adopted, where the E*ffective Aperture* for windows on vertical façades is calculated as the product of the VLT value and the proportion of the window area (including framing) to the 'gross wall area' [4,5], which is measured from the top of the floor to the bottom of the roof [9]. The *Effective Aperture* measured on each floor can be expressed in **Eq. (1)**:

$$max\ EA = VLT \cdot \sum_{i=1}^{n} WWR_i \quad (1)$$

where n is the total number of glazed walls on a particular level. VLT and WWR_i correspond to design variables window type and the WWR scheduled for wall i respectively.

3.3. Computing summer heat gain and winter heat loss

Heat gain and heat loss via solar radiation and conduction are functions of window properties and the window size, and the equations are generally formulated as given in **Eq. (2)** [42] and **Eq. (3)** [80] respectively:

$$HG' = SHGC \cdot WA \cdot I \quad (2)$$

$$HL' = U \cdot WA \cdot \Delta T \quad (3)$$

In these two equations, WA is the total window area on each story, I is the solar irradiance, and ΔT is the indoor and outdoor temperature difference. Solar irradiance and temperature difference are two factors that are highly dependent on real operating conditions.

Solar irradiance can vary significantly according to the seasonal solar angle [66] and window orientations [18], and can also be manipulated by changing window positions and adding shading devices. In other studies, this parameter relies on simulation results or direct measurement to form the basis of calculation, for example, see [34, 45]. The value of ΔT in previous studies is often assumed as a constant based on local construction compliances [8].

In this study, in order to calculate *Summer Heat Gain* and *Winter Heat Loss*, a term *Exposure Factor* introduced in NCC [54] is adopted. *Exposure Factors* are a range of coefficients representing windows'

Preprints (www.preprints.org) | NOT PEER-REVIEWED | Posted: 6 October 2020 doi:10.20944/preprints202010.0111.v1

exposure to the sun for different building orientations in heating and cooling seasons respectively across all climate zones in Australia [54]. For a given climate zone and orientation, *Exposure Factors* for summer and winter design considerations are associated with a term $\frac{p}{h}$, where when the width of the shading device p and the wall geometries are constants, *Exposure Factors* on each wall are only dependent on window placement height, calculated as the total wall height minus h, which is measured from the base of the window to the bottom of the shading device. Therefore, we can deal with discrete *Exposure Factors* instead of the continuous window height variables in the optimisation. **Fig. 2** demonstrates how *Summer Exposure Factor* for east and southeast-facing windows can be associated with a series of $\frac{p}{h}$ coefficients. The $\frac{p}{h}$ values are also indexed in an ascending order to facilitate retrieving data in the optimisation process.

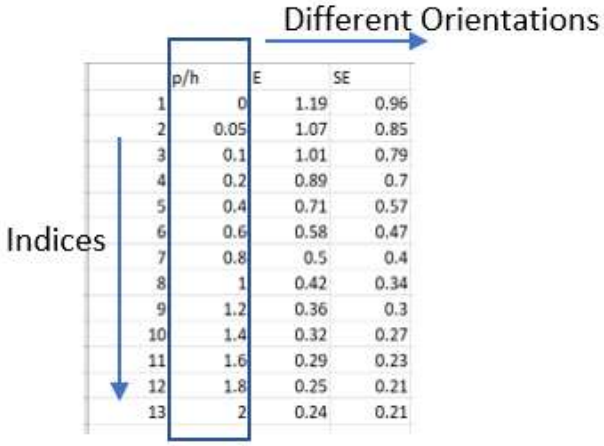

	p/h	E	SE
1	0	1.19	0.96
2	0.05	1.07	0.85
3	0.1	1.01	0.79
4	0.2	0.89	0.7
5	0.4	0.71	0.57
6	0.6	0.58	0.47
7	0.8	0.5	0.4
8	1	0.42	0.34
9	1.2	0.36	0.3
10	1.4	0.32	0.27
11	1.6	0.29	0.23
12	1.8	0.25	0.21
13	2	0.24	0.21

Figure 2 - Example of Associating Exposure Factors to p/h Values

Summer Heat Gain and *Winter Heat Loss* on each level draw upon the aggregate heat gain and aggregate conductance equations given in NCC [54]. As such, objective functions shown in **Eq. (4)** and **Eq. (5)** respectively are defined:

$$min\ HG = SHGC \cdot \sum_{i=1}^{n} ES_i \cdot WWR_i \cdot A_i \quad (4)$$

$$min\ HL = \frac{U}{SHGC} \cdot \frac{\sum_{i=1}^{n} WWR_i \cdot A_i}{\sum_{i=1}^{n} EW_i \cdot WWR_i \cdot A_i} \quad (5)$$

where A_i is the gross area of a glazed wall, and by multiplying it and WWR_i, the glazing area on a wall is calculated. ES_i and EW_i denote the *Summer Exposure Factor* and *Winter Exposure Factor* adopted. ES_i and EW_i are design variables obtained from two reference tables for *Summer Exposure Factors* and *Winter Exposure Factors* respectively, which are originally obtained from the NCC and stored in CSV files following the table format shown in **Fig. 2** Note that for $\frac{p}{h}$ values that are not present in the table, the next lowest $\frac{p}{h}$ value will be adopted for identifying an ES_i, while the next highest $\frac{p}{h}$ will be adopted for *Winter Exposure Factors* for more stringent results [54]. This will provide us with discrete height ranges at the end of the optimisation process. In these equations, $SHGC$ and U are associated to the same window type as VLT. **Eq. (4)** aims to minimize the heat gain in summer, while **Eq. (5)** conveys the strategy of leveraging beneficial winter heat gain to offset heat loss.

3.4. Model constraints

As discussed earlier, three classes of constraints are defined in the proposed optimisation framework. The first constraint class defines the model boundaries for window placement. The second constraint class prevents overglazing. The third constraint class imposes a maximum value allowed for *Summer Heat Gain* and *Winter Heat Loss*, respectively.

Preprints (www.preprints.org) | NOT PEER-REVIEWED | Posted: 6 October 2020 doi:10.20944/preprints202010.0111.v1

3.4.1. Window placement constraint

This constraint class refers to the underlying design requirement that there exists a height range on each wall that is feasible for installing a window. Considering the functionality of windows and the design feasibility, two considerations are accounted for: (i) windows should be placed above a certain working plane; and (ii) a minimum distance that is proportional to a scheduled WWR should be maintained at the top of the wall to prevent design clashes. These two constraints are defined in **Eq. (6)** and **Eq. (7)** respectively:

$$\underline{WH_i}=H_i - WP \quad (6)$$

$$\overline{WH_i}=H_i - H_i \cdot WWR_i \quad (7)$$

where $\underline{WH_i}$ and $\overline{WH_i}$ represent the lowest and highest placement points for positioning a window on a wall, H_i is the height of the hosting wall given as a predefined parameter. The height of the working plane, WP is to be determined by the designer.

3.4.2. Window-to-Floor Ratio (WFR) constraint

Eq. (8) specifies a restriction on the total glazed areas on each floor by setting a lower and upper bound for the *WFR*, to ensure feasible design. F is the fully enclosed covered area of the corresponding floor, and hence the *WFR* indicates the proportion of floor to be heated via the glazing system. Designers have the liberty to determine the inputs of the maximum and minimum *WFR*, represented by $\overline{WFR}$ and $\underline{WFR}$.

$$\underline{WFR} \leq \frac{\sum_{i=1}^{n} WWR_i \cdot A_i}{F} \leq \overline{WFR} \quad (8)$$

As the tolerance to *WFR* varies depending on the daylight factor and exterior illuminance level in the local context [90], as a general guideline, the *WFR* adopted can be as low as 10% [54, 58], and can also go up to 50% [90] in some studies.

3.4.3. Maximum thermal values constraint

NCC Volume Two outlines design requirements for the maximum aggregate heat gain and aggregate conductance, allowed for residential houses [54], which are the basis for the formulation of *Summer Heat Gain* and *Winter Heat Loss* in this study. Considering the similarities in energy use and thermal performance in all residential dwellings [57], this paper applies the same set of compliance to other residential buildings under the research scope to achieve more realistic optimisation results.

The maximum values allowed for *Summer Heat Gain* and *Winter Heat Loss* are given in **Eq. (9)** and **Eq. (10)** below, where C_{SHGC} and the C_U are deemed-to-satisfy constants offered in NCC for residential building in different climate zones [54].

$$\overline{HG} = F \cdot C_{SHGC} \quad (9)$$

$$\overline{CON} = C_U \quad (10)$$

In these equations, F is the floor plate area on each floor. **Eq. (9)** is the maximum value allowed for *Summer Heat Gain* given in **Eq. (4)**, and **Eq. (10)** nominates a constant C_U as the upper bound on **Eq. (5)**.

Preprints (www.preprints.org) | NOT PEER-REVIEWED | Posted: 6 October 2020 doi:10.20944/preprints202010.0111.v1

3.5. Penalty function

Two different approaches are adopted to handle the constraints identified above. **Eq. (7) - (10)** are imposed using penalty functions. This can be achieved because they are either restricting the objective function values or are dependent on optimisation variable selection. The lower bound of the Window Placement Constraint as in **Eq. (6)** is specified via design inputs.

Given that any violation on optimisation constraint would yield equally unfeasible design, in this study penalties are applied without distinguishing the level of violations or the number of violations. To achieve this, a structure that is suitable to implement in Optimo is proposed to evaluate and penalize unfit results, see **Fig. 3**. Note that although the evaluation of the *Summer Heat Gain* and *Winter Heat Loss* objective functions is expressed using one logical path, their evaluation process is independent.

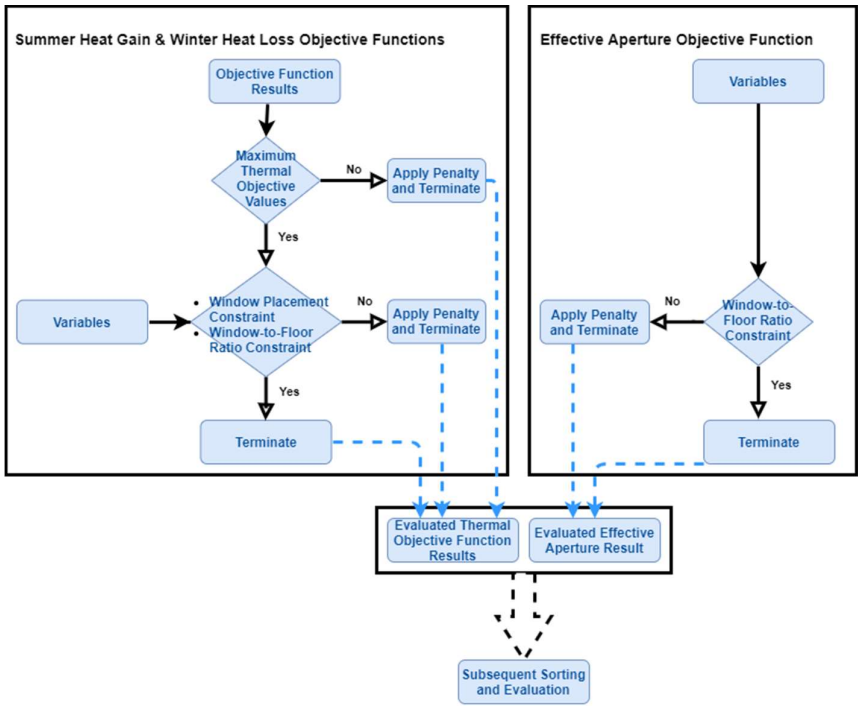

Figure 3 - Penalty Function Structures

Once the *Summer Heat Gain* and *Winter Heat Loss* objective function results are obtained, they are first compared with the Maximum Thermal Objective Values defined in **Eq. (9)** and **Eq. (10),** respectively; if any violation occurs, a constant penalty, denoted as P, will be applied to the offending objective function value, leading to a termination of its evaluation process at this generation. The performance of the *Summer Heat Gain* and *Winter Heat Loss* objective values are represented using binary variable δ_g and δ_l,respectively, which will equal 1 if there is any violation. Further examination on design variables against the upper bound of the Window Placement Constraint and WFR Constraint would be executed if the preceding Maximum Thermal Objective Value is respected, meaning that the corresponding δ_g or δ_l is equal to 0. The Boolean expressions for the Window Placement Constraint and the WFR Constraint are represented using two binary variables δ_h and δ_f respectively; for either *Summer Heat Gain* or *Winter Heat Loss*, any violation on these two conditions would impose the same constant penalty P. The *Effective Aperture* value is examined in a similar but more straightforward fashion with only the WFR Constraint assessed. At each generation, only the evaluated objective function results could continue with the NSGA-II nondominated sorting and reproduction process [90]. Therefore, the proposed penalty function structure can be expressed using **Eq. (11) - (13):**

Preprints (www.preprints.org) | NOT PEER-REVIEWED | Posted: 6 October 2020 doi:10.20944/preprints202010.0111.v1

$$f_{p1}(HG) = \delta_g \cdot P + (1 - \delta_g)\big(HG + P \cdot \max(\delta_h, \delta_f)\big) \quad (11)$$

$$f_{p2}(HL) = \delta_l \cdot P + (1 - \delta_l)\big(HL + P \cdot \max(\delta_h, \delta_f)\big) \quad (12)$$

$$f_{p3}(EA) = EA + P \cdot \delta_f \quad (13)$$

Let $f_{p1}(\mathrm{HG})$ and $f_{p2}(\mathrm{HL})$ be the penalty function for *Summer Heat Gain* and *Winter Heat Loss* described above, and $f_{p3}(\mathrm{EA})$ aims to evaluate *Effective Aperture*. P is the constant penalty 1000. δ_g, δ_l, δ_h and δ_f are binary variables representing four possible situations the algorithm might encounter, i.e. whether HG and HL exceed the maximum values allowed and the violation on the Window-to-Floor Ratio Constraint and the upper bound of Window Placement Constraint.

3.6. Dynamo Workflow

To execute the proposed framework, a Dynamo workflow illustrated in **Fig. 4-6** has been developed. The structure corresponds to the framework shown in **Fig. 1**. Main components at each stage are grouped under their respective labels.

In **Fig. 4**, under *Optimisation Variables*, users are asked to choose the file path where design variables are stored. It is expected that available design variables are prepared a priori and saved in CSV file format. Similarly, users are also required to select window hosting walls as highlighted in *Optimisation Parameters*. **Fig. 4** illustrates an example of selecting four glazed walls.

Data read from designated CSV files and extracted geometries in **Fig. 4**. will be input to *Fitness Functions*, see *Fitness Function Lists* in **Fig. 5.** Each *Fitness Function* comprises one of the design objectives discussed earlier together with penalty functions to restrict variables involved. However, *Fitness Functions* will not be able to retrieve variables without the commands labelled under *Generating and Sorting* to obtain the variable ranges specified in *Optimo Configuration*. In addition, *Generating and Sorting* contains the main body of the NSGA-II algorithm for sorting and evaluating *Fitness Function* results.

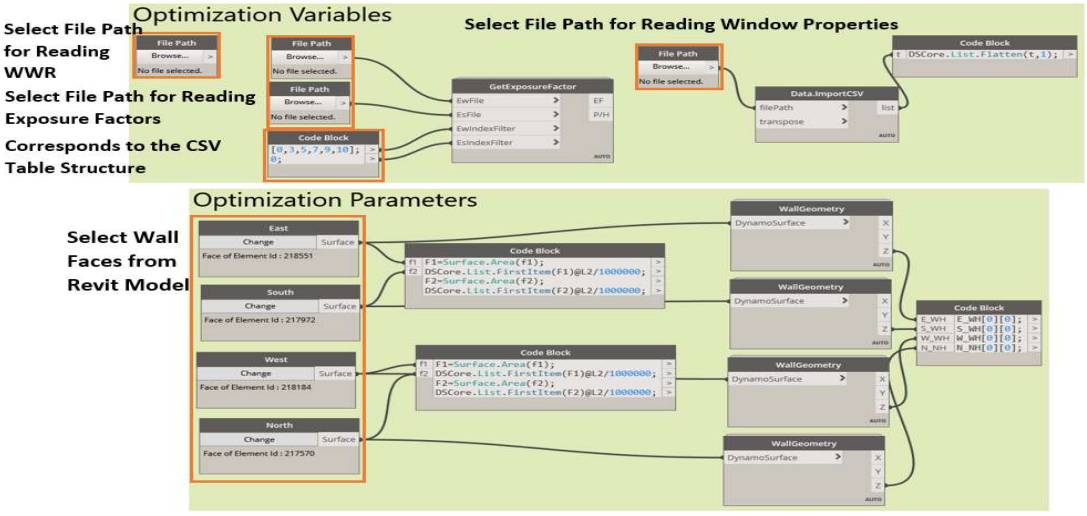

Figure 4 - Dynamo Workflow of Obtaining Optimisation Inputs and Parameters

Preprints (www.preprints.org) | NOT PEER-REVIEWED | Posted: 6 October 2020 doi:10.20944/preprints202010.0111.v1

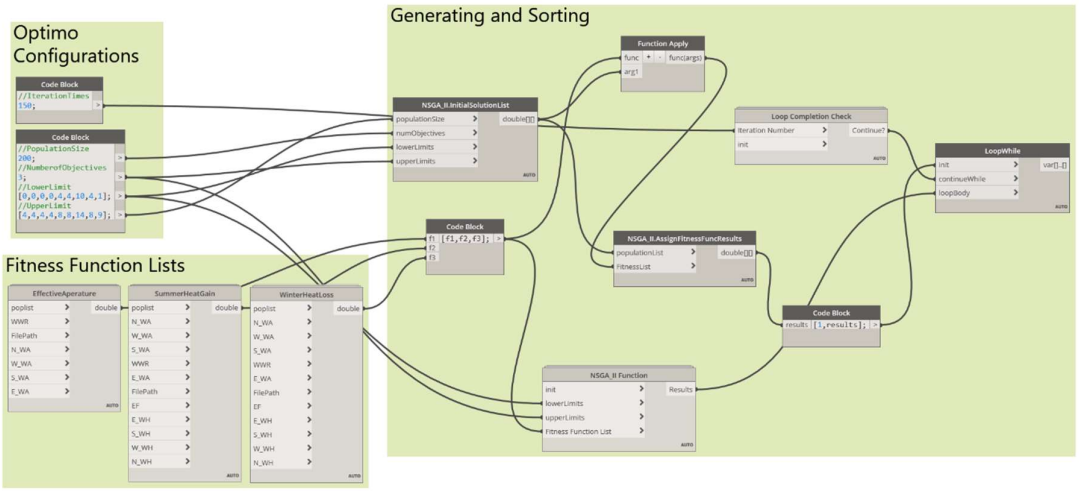

Figure 5 - Dynamo Workflow of Optimisation Setup and Fitness Functions

Fig. 6 illustrates the workflow of preparing the data for plotting the parallel coordinates. This graph enables us to visualize three design objectives in a 2-dimensional space by plotting all design attributes as parallel lines [16]. As this optimisation problem involves multiple design criteria for consideration, this presentation offers a more compact way to view and compare different designs. An iterative data exportation for 3-dimensional scatter plot is achieved by including relevant codes under each *Fitness Functions*. Since some design variables, such as window type and WWR, including the window height variable, could be presented as discrete values in the Optimisation, each variable is handled an index by Optimo, and *Retrieve Associated Variable* is where 'real' variable values are retrieved from the original CSV file.

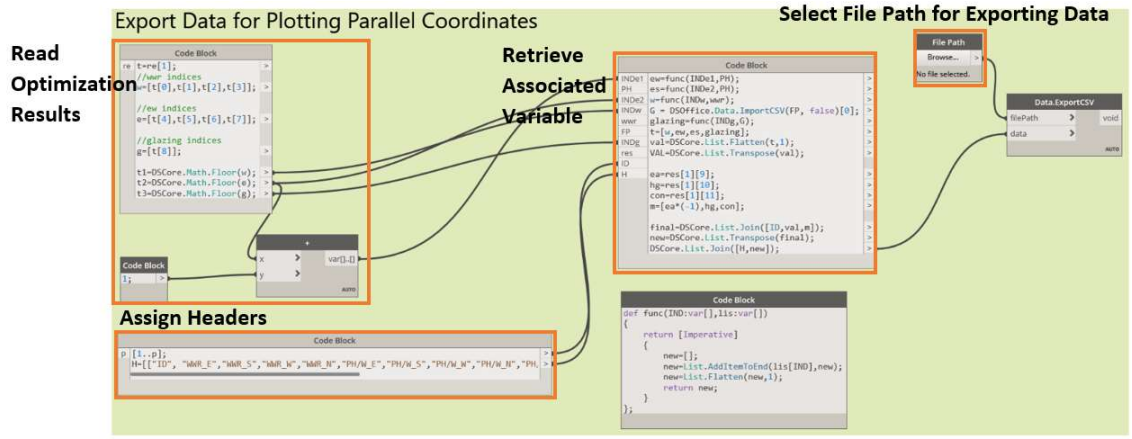

Figure 6 - Dynamo Workflow of Exporting Data for Plotting Parallel Coordinates

4. Case Study

In order to demonstrate the applicability of the framework proposed herein, a case study of a realistic single-story house is examined in Dynamo using the proposed optimisation framework. Minor modifications were made to the BIM model for confidentiality reasons. As seen in **Fig. 7**, the house is facing west and has a verandah and eaves for shading purposes. **Fig. 8** indicates the plan view. The total area of the building is 59.4m^2. A WWR of 55% and 45% are scheduled for its west and north façade, respectively, and its southern and eastern facing walls have a WWR of 50%. All windows are clear single glazing with aluminum framing and designed with a sill height of 500mm.

Preprints (www.preprints.org) | NOT PEER-REVIEWED | Posted: 6 October 2020 doi:10.20944/preprints202010.0111.v1

Australian regions are categorised under eight climate zones: (i) Zone 1 – high humidity summer, warm winter; (ii) Zone 2 – warm humid summer, mild winter; (iii) Zone 3 – hot dry summer, warm winter; (iv) Zone 4 – hot dry summer, cool winter; (v) Zone 5 – warm temperature; (vi) Zone 6 – mild temperature; (vii) Zone 7 – cool temperature; and (viii) Zone 8 – Alpine. The project is located in a South-Western suburb of Sydney and is within climate zone 5 (warm temperate) [12].

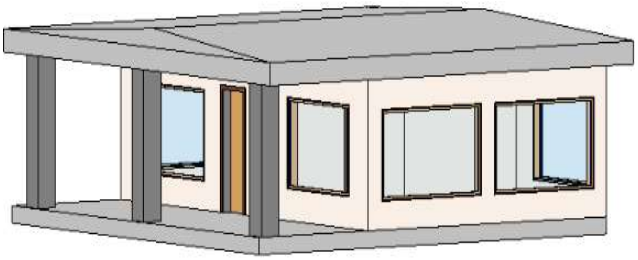

Figure 7 - Visualization of the Base Case

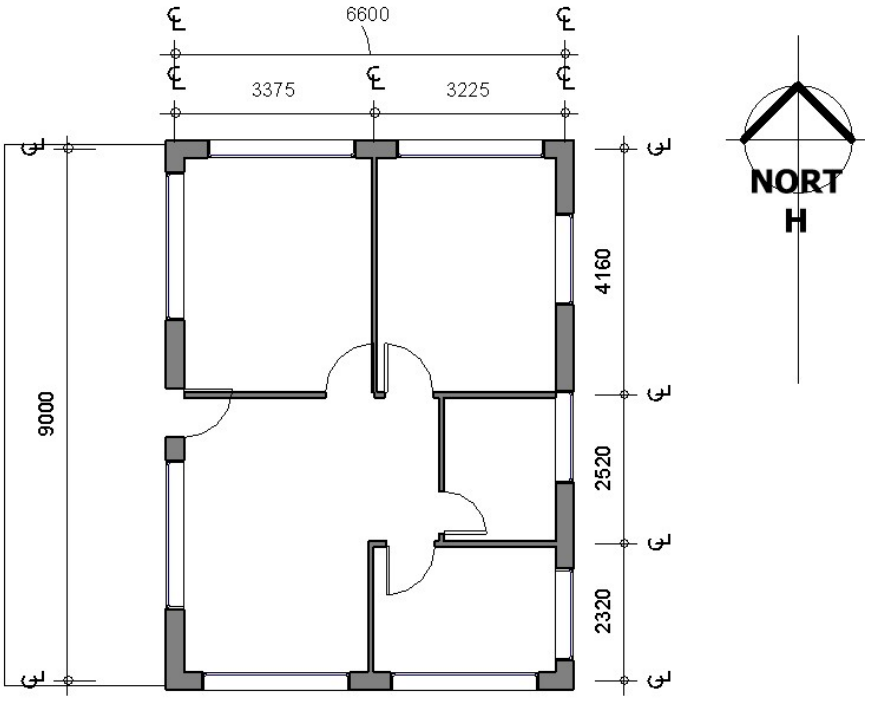

Figure 8 – Floor Plan

4.1. Varaible selection

In many building design optimisation models, continuous variables are commonly used as they are often computationally easier to deal with compared to discrete variables [59]. However, continuous variables sometimes cannot well represent real design practices [87]. In the proposed window design problem, all design criteria were input as discrete variables to represent realistic solutions possible in industry practice. At Stage 1 as shown in **Fig. 1**, variable acceptable ranges were therefore defined according to their associated indices.

Window types used for this case study were obtained from the list of 88 Default Windows [13], which is developed by Australian Fenestration Rating Council to represent performances of glazing products in the market. Four commonly used clear glass windows, namely aluminum windows or

 doi:10.20944/preprints202010.0111.v1

timber/uPVC windows with either single or double glass panels [31], and their four tinted alternatives were selected and the associated properties for the glazing and framing system are shown in Table 3. As the window operating type may have an influence on the vision area, the values adopted are based on double hung, sliding, fixed and louvre windows [13].

Four WWR values tested range from 20% to 50%, and this variable was incremented at a 10% interval. This was adopted with reference to a previous study that investigated the WWR of 20%, 30%, 40% and 80% on a hypothetical residential building in Sydney [81]. The study found significant influence on cooling energy consumption by increasing WWR. In this paper, considering it is recommended to reduce the WWR to a maximum of 50% for Sydney residential buildings [67], the highest input glazing ratio was set as 50%.

An initial height range for window placement was also defined. A horizontal reference work plane, which is usually taken as 750mm in Australia [42], is assumed for this case study. The maximum window placement height was determined based on the minimum possible WWR of 20% and the hosting wall height. Corresponding *Exposure Factors* for each initial height range can therefore be extracted. In addition, a WFR range of 10% to 40% is adopted to restrict glazing areas. A general design rule of thumb for WFR is 20% to 25%, whereas this does not factor in the impacts of the geographical locations of different projects [35]. In this study, the lower bound 10% is a threshold for natural lighting requirement clearly stated in the NCC Volume Two [54]. Although there is no empirical data that specifies an allowance for WFR in Sydney region, a 10% average daylight factor, which is considered as the maximum allowed for the interior [86], was obtained by Ibrahim & Hayman [35] when the WFR is between 30% to 40% in Sydney. In the interest of brevity, this case study took 40% as the upper bound. However, it is acknowledged that setting 40% as the allowance is prone to yield larger than usual WFR. This highlights the importance for designers to determine such data as per project requirements.

Each design option shown in Table 3 has been associated with an index and Table 4 gives the variable range input in Optimo based on the indices.

Table 3 - Case Study Variables

DESIGN VARIABLES

WINDOW TYPE		VLT	SHGC	U-Value
	Single Glazed Clear/Aluminum	0.68	0.7	6.7
	Single Glazed Tint/Aluminum	0.58	0.49	6.6
	Single Glazed Clear/Timber / uPVC / Fiberglass	0.63	0.63	5.4
	Single Glazed Tint/Timber / uPVC / Fiberglass	0.6	0.49	5.4
	Double Glazed Clear/Clear Air Fill/Aluminum	0.57	0.59	4.8

Preprints (www.preprints.org) | NOT PEER-REVIEWED | Posted: 6 October 2020 doi:10.20944/preprints202010.0111.v1

	Double Glazed Tint/Clear Air Fill/Aluminum	0.49	0.39	5.2
	Double Glazed Clear/Clear Air Fill; Timber / uPVC / Fiberglass	0.57	0.56	3
	Double Glazed Tint/Clear Air Fill; Timber / uPVC / Fiberglass	0.37	0.42	2.9
WWR	20%	30%	40%	50%
HEIGHT RANGE	**East Facing**	**South Facing**	**West Facing**	**North Facing**
	750mm-2120mm	750mm-2120mm	750mm-2120mm	750mm-2120mm

Table 4 - Optimo Variable Inputs

Design variable	Optimo Variable Input	Initial Variable Input Ranges	
		Lower Bound	Upper Bound
WWR	East Wall WWR Index	0	4
	South Wall WWR Index	0	4
	West Wall WWR Index	0	4
	North Wall WWR Index	0	4
WINDOW PLACEMENT HEIGHT	East Wall Exposure Factor Index	4	8
	South Wall Exposure Factor Index	4	8
	West Wall Exposure Factor Index	10	14
	North Wall Exposure Factor Index	4	8
Window Type	Window Type Index	1	9

Fig. 9-10 below provide examples of scheduling different WWR for the western/eastern and southern/northern wall faces, where glazing systems are all placed at a minimum sill height of 75cm.

Preprints (www.preprints.org) | NOT PEER-REVIEWED | Posted: 6 October 2020 doi:10.20944/preprints202010.0111.v1

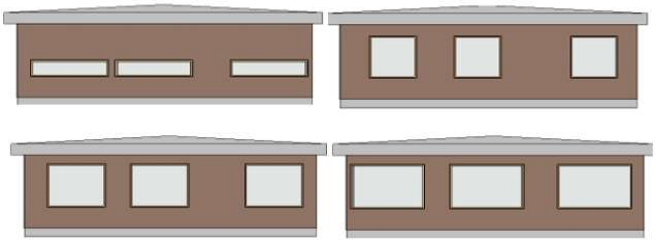

Figure 8 - Illustrative Example for Windows Placed at 750mm above the Floor on North/South-facing Wall. Elevations from Top Left to Bottom Right Indicate a WWR of 20%, 30%, 40%, and 50%.

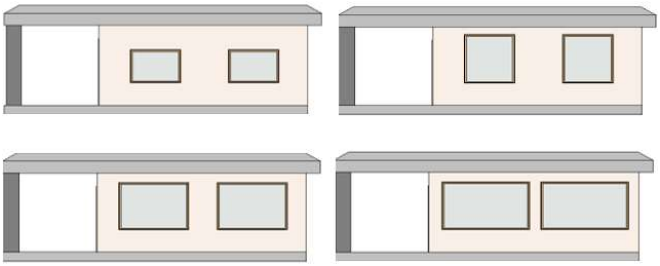

Figure 9 - Illustrative Example for Windows Placed at 750mm above the Floor on West/East-facing Wall Elevations from Top Left to Bottom Right Indicate a WWR of 20%, 30%, 40% and 50%.

4.2. Results and discussion

The calculation process was conducted on a personal computer with a 2.5 GHz processor and 8 GB of RAM in Windows 10 environment. The mutation and crossover probability were set as 0.01 and 0.9, respectively. The distribution indices for crossover and mutation are 20 [70]. In this study, the Pareto Front was obtained after 150 iterations with a population size of 200. The whole process, including exporting approximately 100,000 data points, was completed within 30 mins. **Fig. 11** indicates the evolution of objective function values through generations. Generally , as the process approaches the end of the optimisation, the color of the points displayed exhibits a red color scheme. The Pareto Front generated is presented in **Fig. 12**, where the red points represent optimum design solutions. In this graph, the *Effective Aperture*, *Summer Heat Gain* and *Winter Heat Loss* correspon to the X, Y and Z axis, respectively. One sample point is highlighted below, which has an *Effective Aperture* value of 0.441, a *Summer Heat Gain Value* of approximately 4.03 and a *Winter Heat Loss* value of 2.13 after rounding up.

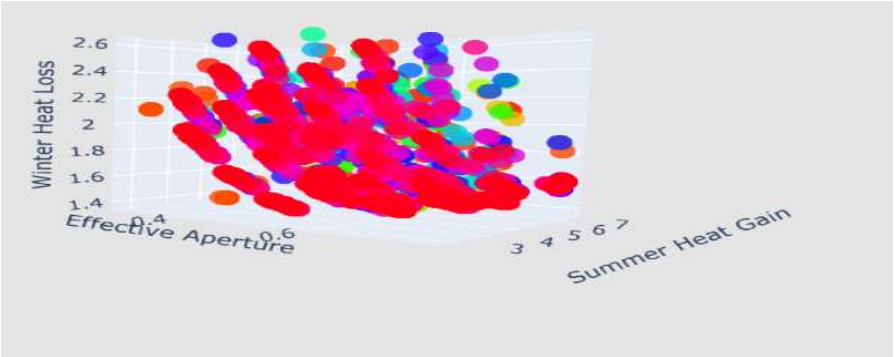

Figure 10 - Improvements of Design Solutions through Evolution

Preprints (www.preprints.org) | NOT PEER-REVIEWED | Posted: 6 October 2020 doi:10.20944/preprints202010.0111.v1

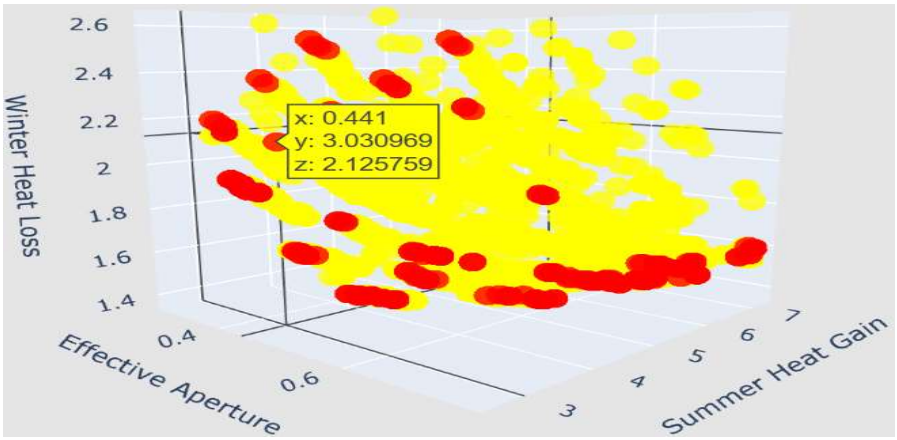

Figure 11 - 3D Pareto Front

Fig. 13 a-c are projections of the Pareto Front onto two design objectives. Fig.**13a** indicates the efficacy of using winter heat gain to compensate heat loss in a warm temperate climate. Fig.**13b** and Fig.**13c** depict the relationship between *Effective Aperture* and windows' thermal performance in summer and winter, respectively. It is observed in Fig.**13b** that a positive relationship exists between the *Effective Aperture* and *Summer Heat Gain*, which is in line with previous findings on *Effective Aperture*'s effect on increasing cooling load [37, 79]. Fig.**13c** shows a more dynamic relationship between the *Effective Aperture* and *Winter Heat Loss*, where the effect of solar gain illustrated in Fig.**13a** also comes into play. Further to this, when controlling *Effective Aperture*, both Fig.**13b** and Fig.**13c** have shown that solar gain and heat loss can be modified by changing the window height. One way to understand Fig.**13b** and Fig.**13c** is by investigating some sample datapoints labelled as group A in Fig.**13a**. It can be deduced that group A represents the optimum designs when only considering the objective of minimizing *Summer Heat Gain* and *Winter Heat Loss* as no smaller value of either of these two objectives can be found while maintaining the performance of the other objective. Seventeen datapoints are captured in group A. The same series of data have also been highlighted in Fig.**13b** and Fig.**13c** as group B and C, respectively. Among the 17 designs, it is found that they are all scheduled with tinted double glazing with aluminum framing and adopt the same WWR strategies, namely, 20% to eastern, southern and western façade, and a 40% to the northern wall. Review **Eq. (1)** for calculating the *Effective Aperture*, and it can be concluded that different values on Y-axis shown in group B and C are only attributed to different window placement heights. The remaining points that have the same *Effective Aperture* values might be a result of the interaction of these three variables.

Figure 13a - Summer Heat Gain and Winter Heat Loss

Preprints (www.preprints.org) | NOT PEER-REVIEWED | Posted: 6 October 2020 doi:10.20944/preprints202010.0111.v1

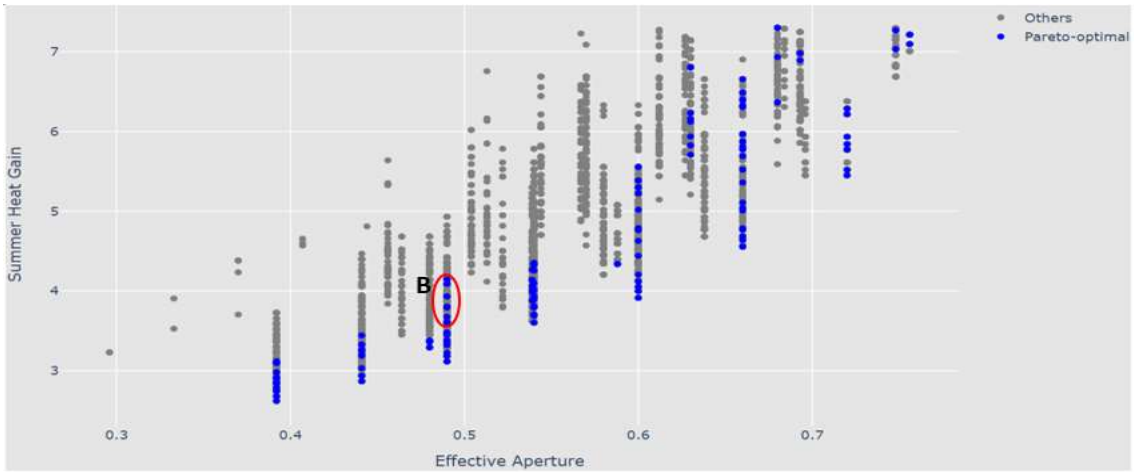

Figure 13b - Effective Aperture and Summer Heat Gain

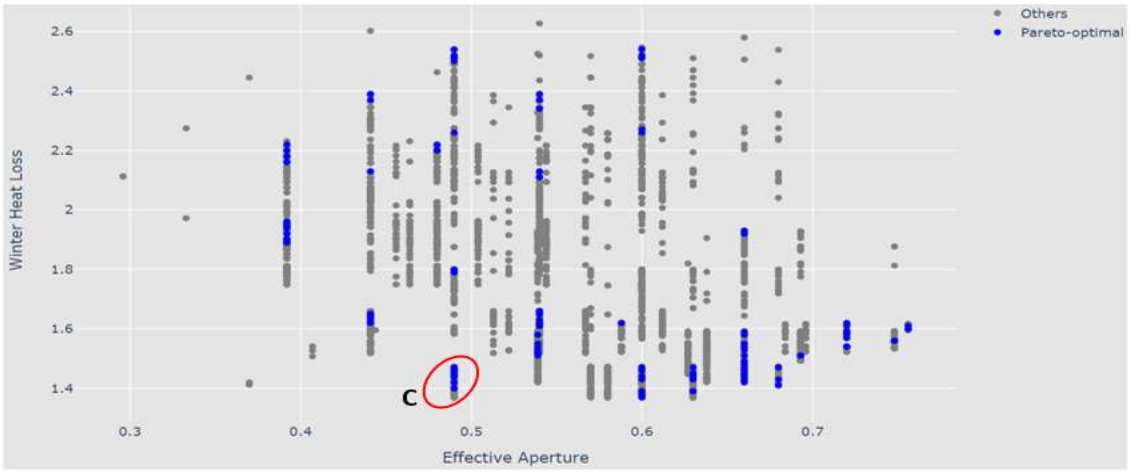

Figure 12c - Effective Aperture and Winter Heat Loss

After removing six penalized values, there were 194 individuals that remained in the final generation. **Fig. 14** and **Fig. 15** take a closer look at the optimum height range and WWR for different wall faces. It is noted that two different strategies to optimize windows' thermal performance can be observed from the Pareto Front. One is the common approach of minimizing glazed area on northern façade in Southern Hemisphere and placing windows at the top part of the wall to avoid heat gain. Another strategy, which has been proven to be effective according to **Fig. 13a**, is to encourage sufficient solar penetration from north-facing wall to reduce winter heat loss. Installing windows at lower heights would exaggerate this effect. As such, the intense solar radiation from the north is fully used as an alternative to mechanical heating in winter, savings from which in theory may potentially offset the additional summer cooling expenditure induced. Among all 194 solutions, around 87% of the total favour this strategy by positioning northern windows at a lower height (750mm – 1525mm), and more than half of the designs also offer generous glazing areas to the north. In addition, noting that optimum design solutions tend to allocate relatively small windows (<30%) to east, south and west-facing walls; this is reported in all cases for eastern façade and around 90% for southern and western façade. This is in line with the strategy of taking advantage of sunlight from the north while designing small windows to these three orientations only for cross-orientation purpose [65]. It is also observed that no WWR of 50% was recorded in the Pareto Front. One possible explanation is WFR shown in **Eq. (8)** plays a prominent role in restricting the total window area.

Preprints (www.preprints.org) | NOT PEER-REVIEWED | Posted: 6 October 2020 doi:10.20944/preprints202010.0111.v1

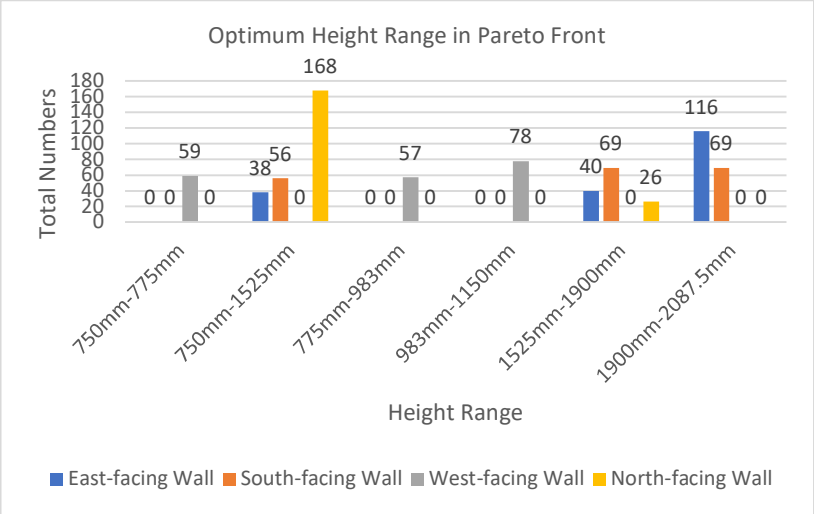

Figure 13 - Optimum Window Height Range on Different Walls

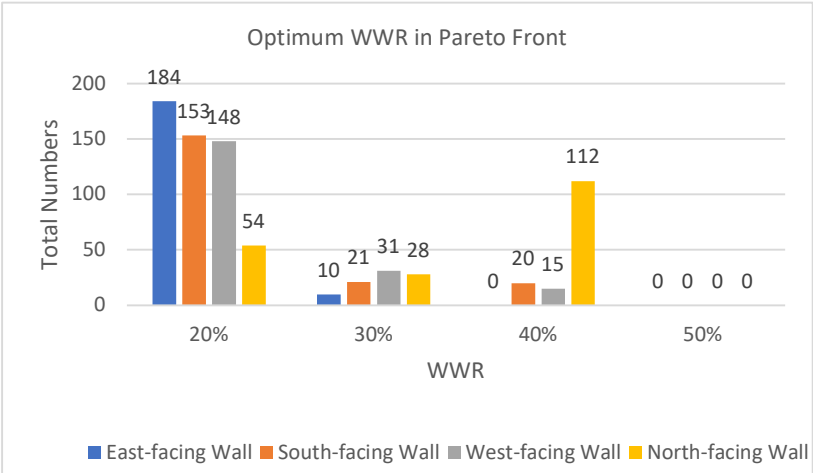

Figure 14 - Optimum WWR on Different Walls

Four solutions that obtained a single optimum value were identified as a sample of the Pareto Front. The detailed window design options offered by these four designs are presented in **Table 4**. Optimum window design attributes have been plotted using parallel coordinates to display a clear design trade-off, see **Fig. 16**, where solution A, B, C, and D are represented using different colours. All solutions have a WWR of 20% scheduled for the east and west-facing wall. Design A aims to minimize *Winter Heat Loss* by placing better thermally insulated timber framed windows at lower parts of the wall to allow for more solar penetration in winter. In addition, generous window area is scheduled for north-facing wall to capture winter solar radiation. On the contrary, design B tends to limit the window size and window placement points are higher in order to avoid direct exposure to the sun. Double glazing with low SHGC value is selected to eliminate unwanted heat gain. Design C and D are focusing on optimizing the *Effective Aperture* requirement by employing glazing with high VLT value and average thermal performance and assigning large window areas to the south.

Preprints (www.preprints.org) | NOT PEER-REVIEWED | Posted: 6 October 2020 doi:10.20944/preprints202010.0111.v1

Table 5 - Window Design Solutions Chosen from Points on Pareto Front

	WWR	Height Range	WWR	Height Range	WWR	Height Range	WWR	Height Range	
A	0.2	750-1525mm	0.2	750-1525mm	0.2	750-775mm	0.4	750-1525mm	Single Glazed Tint/Timber / uPVC / Fiberglass
B	0.2	1900-2087.5mm	0.2	1900-2087.5mm	0.2	983-1150mm	0.2	1525-1900mm	Double Glazed Tint/Clear Air Fill/Aluminum
C	0.2	1900-2087.5mm	0.4	750-1525mm	0.2	750-775mm	0.4	750-1525mm	Single Glazed Clear/Timber / uPVC / Fiberglass
D	0.2	1900-2087.5mm	0.4	750-1525mm	0.2	775-983mm	0.4	750-1525mm	Single Glazed Clear/Timber / uPVC / Fiberglass

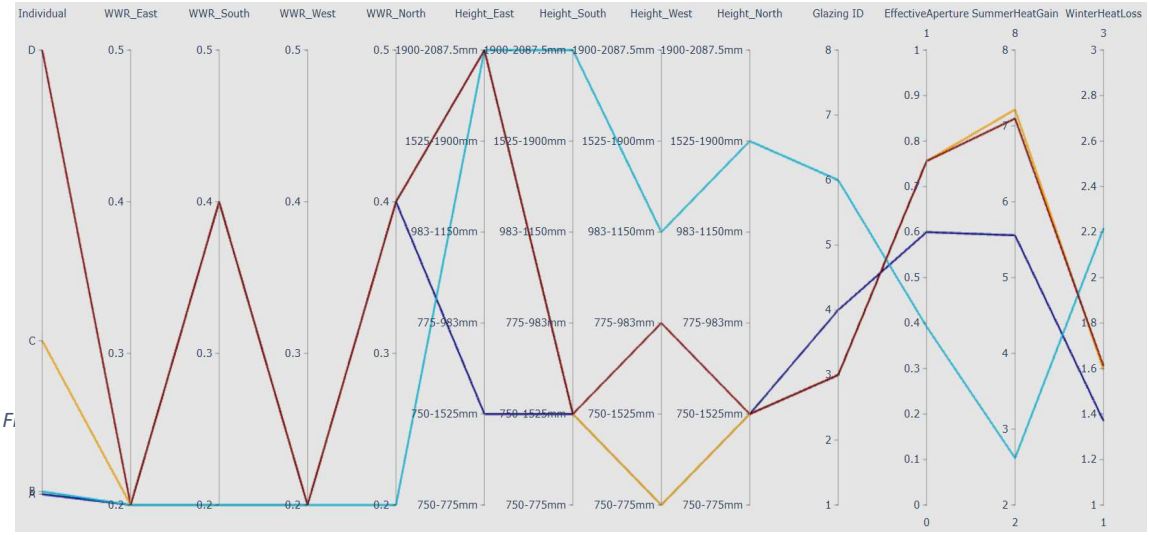

Figure 16 - Parallel Coordinates

Preprints (www.preprints.org) | NOT PEER-REVIEWED | Posted: 6 October 2020 doi:10.20944/preprints202010.0111.v1

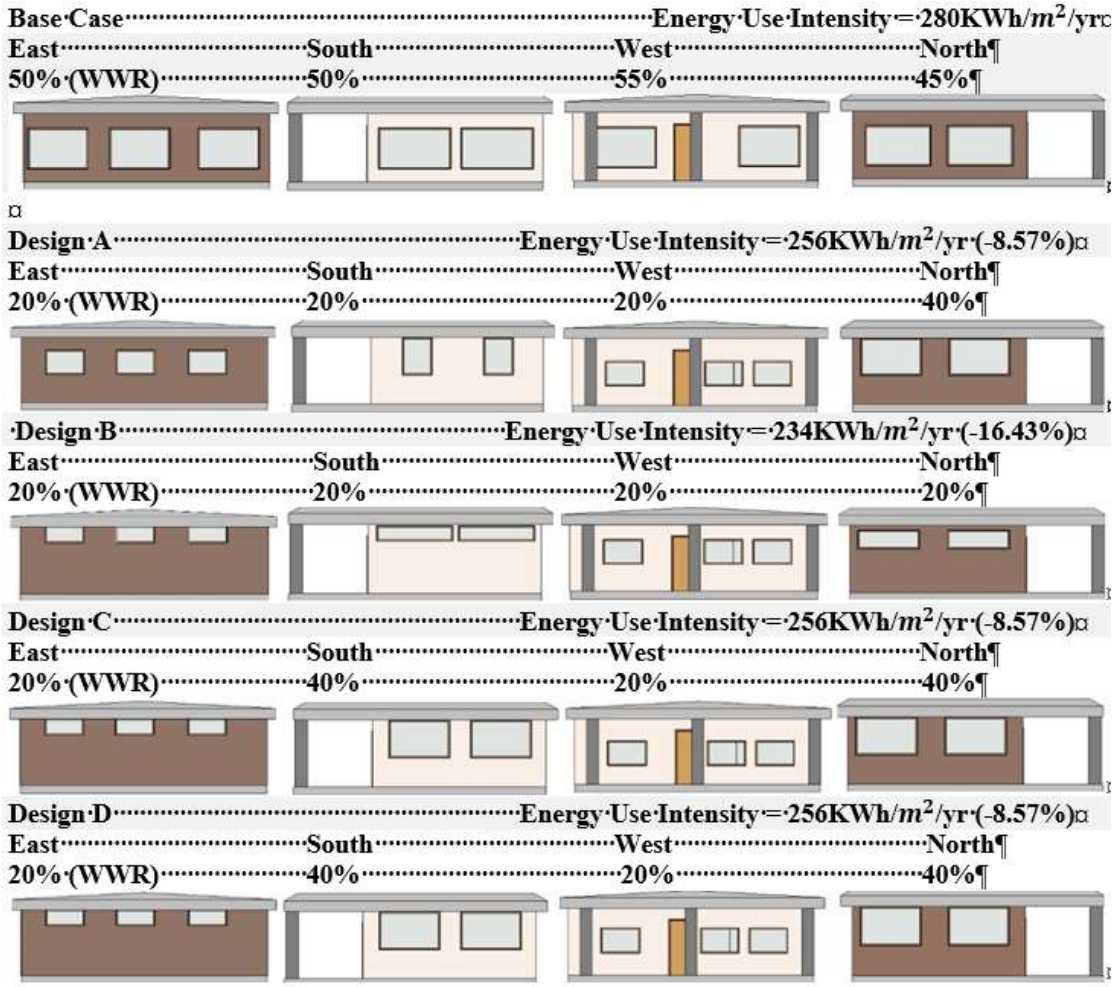

Figure 17 - Illustrative Example of Sample Design A to D

Approximately 8.57% reduction on annual energy consumption is observed for design A, C and D, while this figure has nearly doubled for design B, which emphasizes the passive window design strategy that minimizes *Summer Heat Gain*. This seems to be conflicting with the finding reported earlier on that leveraging winter heat gain to compensate heat loss in Sydney region.

This can be partially explained by the fact that Sydney has a temperate climate and is heating and cooling balanced [88]. When it comes to the total energy consumption, which is the function of summer heat gain, and winter heat loss and effective aperture in this case, extra cooling load induced from generous solar gain might not be fully recovered from reduced use of heating equipment in winter for Sydney. As these sample designs are obtained from the Pareto Front, they all represent equally good practices when controlling other design parameters. Therefore, by contrasting Design A with B, it is informed that over emphasis on the effect of leveraging northern sunlight to offset winter heating could in fact jeopardize the efficacy of the design.

Design A took an opposite design approach compared to Design C and D; small windows are scheduled to the south and tinted glass are installed, while the other attributes are similar. These designs achieved the same energy performance. Again, this corresponds to the findings from **Fig. 13b**, and coincides with the established theory on *Effective Aperture*'s effect on increasing cooling load, which has been discussed earlier on.

5. Conclusions

A window design optimisation problem was proposed in this study for the window type, WWR and window height for residential buildings in non-tropical regions in Australia using a BIM platform, Revit and its extension Dynamo. Three objective functions concerning the natural light, undesirable heat gain in summer and heat loss in winter together with four penalty functions that impose realistic design constraints were formulated and solved using an NSGA-II Optimisation package of Dynamo, Optimo. A range of coefficients offered by the Australian construction regulatory framework, NCC, were adopted to translate the continuous window height variable into discrete values. Architectural model geometries, such as hosting wall areas and heights were extracted from the building model as optimisation parameters.

The results were presented in the form of Pareto Front with the improvements of design objectives throughout the optimisation process visualized using 3-dimensional scatter plot. To further showcase the interplay of different design attributes, a sample of four designs identified from the result set, representing the most ideal solution for each objective, was displayed using parallel coordinates. A Revit energy analysis plugin, Insight, was employed to simulate these four designs to get the annual energy consumption in order to contrast with the base case. The simulation results suggest a maximum of 16.43% energy reduction could be realized when applying the design that focuses on minimizing heat gain in summer.

This novel optimisation framework offers a BIM-integrated approach to deal with a practical window design problem. The findings shed some light on the window design strategy in temperate regions that even though winter sunlight is beneficial, winter sun penetration is not the top design priority as these regions most likely have a balanced heating and cooling requirement. The proposed workflow has demonstrated the feasibility of conducting a numerical-based design optimisation on a common modelling platform, providing an opportunity for integrating optimisation into industry design practice.

That said, one weakness of this work is that the developed framework still requires to be tailored on a project basis for similar window design problems. Furthermore, new *Fitness Functions* need to be formulated from scratch if users are interested in other optimisation scenarios. This is primarily rooted in the identified industry knowledge gap that basic DesignScript and Python are still not common languages. This will hinder the adoption of the propsoed optimisation workflow. Another limitation is that no sensitivity analysis was conducted to understand the role each design parameter played in the window design problem.

Future work built upon this study could involve generalizing the proposed Optimo optimisation framework so that designers only need to choose the file paths for variable input, while the remaining process will be competed automatically. Further to this, the proposed framework could be integrated with the modelling software as an addon and the interaction could be achieved via the use of Application Programming Interface (API), delivering a fully automated optimisation workflow. Similar interaction was realized by Rahmani Asl, Zarrinmehr, et al. [70] by linking an Optimo framework with Green Building Studio for real-time simulation. However, the connection was discontinued [3] due to lack of maintenance, which also sheds light on the importance of continuing collaboration between key industry players and the academia.

Author Contributions: Conceptualization, Z.C. and AWH.; Methodology, Z.C and AWH.; Software, Z.C.; Validation, Z.C., AWH., I.K and A.H.; Formal Analysis, Z.C..; Investigation, Z.C. and AWH.; Resources, Z.C and AWH.; Data Curation, Z.C.; Writing – Original Draft Preparation, Z.C and AWH..; Writing – Review & Editing, Z.C., AWH., IK and A.H.; Visualization, Z.C, AWH. And A.H.; Supervision, AWH. and A.H.; Project Administration, A.W.H and I.K.; Funding Acquisition, A.W.H .

Funding: This research was funded by UNSW Built Environment Limited APC Scheme.

Conflicts of Interest: N/A

References

1. Acosta, I., Campano, M. Á., & Molina, J. F. (2016). Window design in architecture: Analysis of energy savings for lighting and visual comfort in residential spaces. *Applied Energy*, *168*, 493–506. https://doi.org/10.1016/j.apenergy.2016.02.005
2. Aish, R., & Mendoza, E. (2016). DesignScript: A domain specific language for architectural computing. *Proceedings of the International Workshop on Domain-Specific Modeling*, 15–21. https://doi.org/10.1145/3023147.3023150
3. *Alternative GBS Runs Energy Analysis*. (2016, November 29). Dynamo. https://forum.dynamobim.com/t/alternative-gbs-runs-energy-analysis/7823
4. *ANSI/GBI 01-2010 Green Building Assessment Protocol for Commercial Buildings*. (2010). Green Building Initiative. https://thegbi.org/content/misc/GBI_ANSI_procedures_GBI-PRO_2015_-_ANSI_approved_2-4-162.pdf
5. *ANSI/GBI 01-2019 Green Globes Assessment Protocol for Commercial Buildings*. (2019). Green Building Initiative. https://thegbi.org/content/misc/ANSI-GBI_01-2019_Publication_-_final_6-14-19_.pdf
6. Arasteh, D. (1995). Advances in Window Technology: 1973-1993. 49.
7. Arasteh, Dariush, Selkowitz, S., Apte, J., & LaFrance, M. (2006). *Zero Energy Windows*. 14.
8. Asadi, E., da Silva, M. G., Antunes, C. H., & Dias, L. (2012). Multi-objective Optimisation for building retrofit strategies: A model and an application. *Energy and Buildings*, *44*, 81–87. https://doi.org/10.1016/j.enbuild.2011.10.016
9. ASHRAE Standards Committee 2019-2020. (2019). *ANSI/ASHRAE/IES Standard 90.1-2019 Energy Standard for Buildings Except Low-Rise Residential Buildings (I-P Edition)*. American Society of Heating, Refrigerating and Air-Conditioning Engineers, Inc. https://ashrae.iwrapper.com/ViewOnline/Standard_90.1-2019
10. Attia, S., Hamdy, M., O'Brien, L., & Carlucci, S. (2013a, August 28). *Computational Optimisation for Zero Energy Buildings Design: Interview results with twenty-eight International experts*. Proceedings of BS 2013: 13th Conference of the International Building Performance Simulation Association.
11. Attia, S., Hamdy, M., O'Brien, W., & Carlucci, S. (2013b). Assessing gaps and needs for integrating building performance Optimisation tools in net zero energy buildings design. *Energy and Buildings*, *60*, 110–124. https://doi.org/10.1016/j.enbuild.2013.01.016
12. Australian Building Codes Board. (2019). *New South Wales Australian Capital Territory Climate Zone Map*. Australian Building Codes Board. https://www.abcb.gov.au/Resources/Tools-Calculators/Climate-Zone-Map-Australia-Wide
13. Australian Fenestration Rating Council. (2014). *Release of Defaults—AFRC Industry Announcement*. https://www.afti.edu.au/documents/item/735
14. Autodesk. (2020a). *Dynamo*. Dynamo BIM. https://dynamobim.org/download/
15. Autodesk. (2020b). *Insight | Building Performance Analysis Software | Autodesk*. https://www.autodesk.com/products/insight/overview
16. Blasco, X., Herrero, J. M., Sanchis, J., & Martínez, M. (2008). A new graphical visualization of n-dimensional Pareto front for decision-making in multiobjective Optimisation. *Information Sciences*, *178*(20), 3908–3924. https://doi.org/10.1016/j.ins.2008.06.010
17. Bokel, R. M. J. (2007). The Effect Of Window Position and Window Size on The Energy Demand for Heating, Cooling and Electric Lighting. *Building Simulation*, 5.
18. Caldas, L. G., & Norford, L. K. (2002). A design Optimisation tool based on a genetic algorithm. *Automation in Construction*, *11*(2), 173–184. https://doi.org/10.1016/S0926-5805(00)00096-0
19. Chen, X., Yang, H., & Lu, L. (2015). A comprehensive review on passive design approaches in green building rating tools. *Renewable and Sustainable Energy Reviews*, *50*, 1425–1436. https://doi.org/10.1016/j.rser.2015.06.003
20. Cheng, Chengli, Chen, C. L., Chou, C., & Chan, C. Y. (2007). A mini-scale modeling approach to natural daylight utilization in building design. *Building and Environment*, *42*(1), 372–384. https://doi.org/10.1016/j.buildenv.2005.08.004
21. Cheng, Cunyi, Ninic, J., & Tizani, W. (2019, July 5). Parametric Virtual Design-based Multi-Objective Optimisation for Sustainable Building Design.
22. Cheung, C. K., Fuller, R. J., & Luther, M. B. (2005). Energy-efficient envelope design for high-rise apartments. *Energy and Buildings*, *37*(1), 37–48. https://doi.org/10.1016/j.enbuild.2004.05.002
23. Cuce, E. (2017). Role of airtightness in energy loss from windows: Experimental results from in-situ tests. *Energy and Buildings*, *139*, 449–455. https://doi.org/10.1016/j.enbuild.2017.01.027

24. Deb, K., Pratap, A., Agarwal, S., & Meyarivan, T. (2002). A fast and elitist multiobjective genetic algorithm: NSGA-II. *IEEE Transactions on Evolutionary Computation*, *6*(2), 182–197. https://doi.org/10.1109/4235.996017
25. *Energy Conservation Building Code 2017*. (2017). Bureau of Energy Efficiency. https://beeindia.gov.in/sites/default/files/BEE_ECBC%202017.pdf
26. Evins, R. (2013). A review of computational optimisation methods applied to sustainable building design. *Renewable and Sustainable Energy Reviews*, *22*, 230–245. https://doi.org/10.1016/j.rser.2013.02.004
27. Fang, Y., & Cho, S. (2019). Design Optimisation of building geometry and fenestration for daylighting and energy performance. *Solar Energy*, *191*, 7–18. https://doi.org/10.1016/j.solener.2019.08.039
28. Feist, W., Schnieders, J., Dorer, V., & Haas, A. (2005). Re-inventing air heating: Convenient and comfortable within the frame of the Passive House concept. *Energy and Buildings*, *37*(11), 1186–1203. https://doi.org/10.1016/j.enbuild.2005.06.020
29. *Galapagos—Addon for Grasshopper*. (2019, December 15). Grasshopper Docs. c
30. Ghisi, E., & Tinker, J. A. (2005). An Ideal Window Area concept for energy efficient integration of daylight and artificial light in buildings. *Building and Environment*, *40*(1), 51–61. https://doi.org/10.1016/j.buildenv.2004.04.004
31. *Glazing | YourHome*. (2013). https://www.yourhome.gov.au/passive-design/glazing
32. Gong, X., Akashi, Y., & Sumiyoshi, D. (2012). Optimisation of passive design measures for residential buildings in different Chinese areas. *Building and Environment*, *58*, 46–57. https://doi.org/10.1016/j.buildenv.2012.06.014
33. Grynning, S., Gustavsen, A., Time, B., & Jelle, B. P. (2013). Windows in the buildings of tomorrow: Energy losers or energy gainers? *Energy and Buildings*, *61*, 185–192. https://doi.org/10.1016/j.enbuild.2013.02.029
34. Hammad, A., Akbarnezhad, A., Grzybowska, H., Wu, P., & Wang, X. (2019). Mathematical optimisation of location and design of windows by considering energy performance, lighting and privacy of buildings. *Smart and Sustainable Built Environment*, *8*(2), 117–137. https://doi.org/10.1108/SASBE-11-2017-0070
35. Ibrahim, N. L. N., & Hayman, S. (2010). Latitude variation and its influence on rules of thumb in daylighting. *Architectural Science Review*, *53*(4), 408–414. https://doi.org/10.1080/00038628.2010.9685341
36. James J. Hirsch & Associates. (2016). *DOE2.com Home Page*. The Home of DOE-2 Based Building Energy Use and Cost Analysis Software. http://www.doe2.com/
37. Johnson, R., Sullivan, R., Selkowitz, S., Nozaki, S., Conner, C., & Arasteh, D. (1984). Glazing energy performance and design Optimisation with daylighting. *Energy and Buildings*, *6*(4), 305–317. https://doi.org/10.1016/0378-7788(84)90014-8
38. Johnston, D., Zhang, H., Airah, M., Wang, G., Bannister, P., & Airah, F. (2017). *Glazing Studies for The National Construction Code 2019*. 11.
39. Kensek, K. (2015). Visual Programming for Building Information Modeling: Energy and Shading Analysis Case Studies. *Journal of Green Building*, *10*(4), 28–43. https://doi.org/10.3992/jgb.10.4.28
40. Kensek, K. M. (2014). Integration of Environmental Sensors with BIM: Case studies using Arduino, Dynamo, and the Revit API. *Informes de La Construcción*, *66*(536), e044. https://doi.org/10.3989/ic.13.151
41. Kim, S., Zadeh, P. A., Staub-French, S., Froese, T., & Cavka, B. T. (2016). Assessment of the Impact of Window Size, Position and Orientation on Building Energy Load Using BIM. *Procedia Engineering*, *145*, 1424–1431. https://doi.org/10.1016/j.proeng.2016.04.179
42. King, S. (2006). Daylight & Solar Access. Reading between the Lines: Making Sense of Consultant Reports - Understanding the Environmental Sciences Essential to Development Applications. NEERG Seminar: Reading between the lines: making sense of consultant reports - Understanding the environmental sciences essential to development applications; 2006; August, Sydney. http://unsworks.unsw.edu.au/fapi/datastream/unsworks:5026/SOURCE01?view=true
42. Klems, J. (1988). U-Values, Solar Heat Gain, and Thermal Performance: Recent Studies Using the MoWiTT.
44. Kolarik, J., Toftum, J., Olesen, B. W., & Jensen, K. L. (2011). Simulation of energy use, human thermal comfort and office work performance in buildings with moderately drifting operative temperatures. *Energy and Buildings*, *43*(11), 2988–2997. https://doi.org/10.1016/j.enbuild.2011.07.008
45. Kull, T. M., Mauring, T., & Tkaczyk, A. H. (2015). Energy balance calculation of window glazings in the northern latitudes using long-term measured climatic data. *Energy Conversion and Management*, *89*, 896–906. https://doi.org/10.1016/j.enconman.2014.10.058
46. Larson, G. W., & Shakespeare, R. A. (2020). *Rendering with Radiance*. Rendering with Radiance. https://floyd.lbl.gov/radiance/book/index.html

47. Lee, J. W., Park, J., & Jung, H.-J. (2014). A feasibility study on a building's window system based on dye-sensitized solar cells. *Energy and Buildings*, *81*, 38–47. https://doi.org/10.1016/j.enbuild.2014.06.010
48. Levine, M. D., & Busch, J. F. (Eds.). (1992). *Building Energy Conservation Project* (Volume II: TECHONOLOGY). Energy Analysis Program, Energy and Environment Division, Lawrence Berkeley Laboratory, University of California. https://www.osti.gov/servlets/purl/10163215#page=178
49. Li, D. H. W., Lam, J. C., & Wong, S. L. (2005). Daylighting and its effects on peak load determination. *Energy*, *30*(10), 1817–1831. https://doi.org/10.1016/j.energy.2004.09.009
50. Littlefair, P. (2001). Daylight, sunlight and solar gain in the urban environment. *Solar Energy*, *70*(3), 177–185. https://doi.org/10.1016/S0038-092X(00)00099-2
51. Lu, S., Li, Z., & Zhao, Q. (2015). Thermal Process of Windows in Hot Summer and Cold Winter Climate. *Procedia Engineering*, *121*, 1788–1794. https://doi.org/10.1016/j.proeng.2015.09.158
52. Mahar, W. A., Verbeeck, G., Reiter, S., & Attia, S. (2020). Sensitivity Analysis of Passive Design Strategies for Residential Buildings in Cold Semi-Arid Climates. *Sustainability*, *12*(3), 1091. https://doi.org/10.3390/su12031091
53. *National Construction Code Energy efficiency NCC Volume Two*. (2019). Australian Building Codes Board. https://www.abcb.gov.au/Resources/Publications/Education-Training/energy-efficiency-ncc-volume-two
54. *National Construction Code NCC Volume Two*. (2019). Australian Building Codes Board. https://ncc.abcb.gov.au/
55. *National Construction Code Volume 2*. (2019). Australian Building Codes Board.
56. *NCC | Australian Building Codes Board*. (2020). https://ncc.abcb.gov.au/
57. *NCC 2019 Guide to BCA Volume One*. (2019). The Australian Building Codes Board.
58. Nedhal, A.-T., Sharifah Fairuz Syed, F., & Adel, A. (2016). Relationship between Window-to-Floor Area Ratio and Single-Point Daylight Factor in Varied Residential Rooms in Malaysia. *Indian Journal of Science and Technology*, *9*(33). https://doi.org/10.17485/ijst/2016/v9i33/86216
59. Nguyen, A.-T., Reiter, S., & Rigo, P. (2014). A review on simulation-based Optimisation methods applied to building performance analysis. *Applied Energy*, *113*, 1043–1058. https://doi.org/10.1016/j.apenergy.2013.08.061
60. O'Brien, W., Kapsis, K., & Athienitis, A. K. (2013). Manually-operated window shade patterns in office buildings: A critical review. *Building and Environment*, *60*, 319–338. https://doi.org/10.1016/j.buildenv.2012.10.003
61. Ochoa, C. E., Aries, M. B. C., van Loenen, E. J., & Hensen, J. L. M. (2012). Considerations on design Optimisation criteria for windows providing low energy consumption and high visual comfort. *Applied Energy*, *95*, 238–245. https://doi.org/10.1016/j.apenergy.2012.02.042
62. *Octopus*. (2012, December 6). [Text]. Food4Rhino. https://www.food4rhino.com/app/octopus
64. *OpenStudio*. (2020, April 27). https://www.openstudio.net/
65. *Orientation | YourHome*. (2013). https://www.yourhome.gov.au/passive-design/orientation
66. Page, A., Moghtaderi, B., Alterman, D., & Hands, S. (2011). *A study of the thermal performance of Australian housing*. https://nova.newcastle.edu.au/vital/access/manager/Repository/uon:15617
67. Philip, H. (2016). *Accelerating Net-Zero High-Rise Residential Buildings in Australia* (Final Report, p. 9). City of Sydney. https://www.cityofsydney.nsw.gov.au/__data/assets/pdf_file/0005/264398/Accelerating-Net-Zero-High-Rise-Residential-Buildings.pdf
68. Qingsong, M., & Fukuda, H. (2016). Parametric Office Building for Daylight and Energy Analysis in the Early Design Stages. *Procedia - Social and Behavioral Sciences*, *216*, 818–828. https://doi.org/10.1016/j.sbspro.2015.12.079
69. Rahmani Asl, M., Stoupine, A., Zarrinmehr, S., & Yan, W. (2015a). Optimo: A BIM-based multi-objective Optimisation tool utilizing visual programing for high performance building design. *Proceedings of the Conference of Education and Research in Computer Aided Architectural Design in Europe (ECAADe)*, 673–682.
70. Rahmani Asl, M., Zarrinmehr, S., Bergin, M., & Yan, W. (2015). BPOpt: A framework for BIM-based performance Optimisation. *Energy and Buildings*, *108*, 401–412. https://doi.org/10.1016/j.enbuild.2015.09.011
71. Robert McNeel & Associates. (2018, February). *Grasshopper—New in Rhino 6*. https://www.rhino3d.com/6/new/grasshopper
72. Robert McNeel & Associates. (2020). *Rhino Features*. https://www.rhino3d.com/6/features
73. Robinson, A., & Selkowitz, S. (2013). *Tips for daylighting with windows* (LBNL--6902E, 1167562; p. LBNL--6902E, 1167562). https://doi.org/10.2172/1167562
74. Rubin, M. (1982). Calculating heat transfer through windows. *International Journal of Energy Research*, *6*(4), 341–349. https://doi.org/10.1002/er.4440060405
75. Selkowitz, S. (1985). Window performance and building energy use: Some technical options for increasing energy efficiency. *AIP Conference Proceedings*, *135*(1), 258–269. https://doi.org/10.1063/1.35448

76. Shadram, F., & Mukkavaara, J. (2018). An integrated BIM-based framework for the Optimisation of the trade-off between embodied and operational energy. *Energy and Buildings*, *158*, 1189–1205. https://doi.org/10.1016/j.enbuild.2017.11.017

77. Shahbazi, Y., Heydari, M., & Haghparast, F. (2019). An early-stage design Optimisation for office buildings' façade providing high-energy performance and daylight. *Indoor and Built Environment*, *28*(10), 1350–1367. https://doi.org/10.1177/1420326X19840761

78. Statistics, c=AU; o=Commonwealth of A. ou=Australian B. of. (2013, September 24). *Main Features—Climate zone*. c=AU; o=Commonwealth of Australia; ou=Australian Bureau of Statistics. https://www.abs.gov.au/ausstats/abs@.nsf/Lookup/by%20Subject/4671.0~2012~Main%20Features~Climate%20zone~17

79. Sullivan, R., Lee, E., & Selkowitz, S. (1992). A method of optimizing solar control and daylighting performance in commercial office buildings.

80. Szokolay, S. V. (2014). Introduction to Architectural Science: The Basis of Sustainable Design. Routledge.

81. Tabrizi, T. B., Hill, G., & Aitchison, M. (2017). The Impact of Different Insulation Options on the Life Cycle Energy Demands of a Hypothetical Residential Building. *Procedia Engineering*, *180*, 128–135. https://doi.org/10.1016/j.proeng.2017.04.172

82. *The Dynamo Primer*. (2019). Autodesk Dynamo Developmet Team. https://primer.dynamobim.org/index.html

83. Touloupaki, E., & Theodosiou, T. (2017). Performance simulation integrated in parametric 3D modeling as a method for early stage design Optimisation—A review. *Energies*, *10*. https://doi.org/10.3390/en10050637

84. UN Environment and International Energy Agency. (2017). *Towards a zero-emission, efficient, and resilient buildings and construction sector. Global Status Report 2017* (p. 48). International Energy Agency (IEA). https://www.worldgbc.org/sites/default/files/UNEP%20188_GABC_en%20%28web%29.pdf

85. UNEP DTIE Sustainable Consumption & Production Branch. (2009). *Buildings and Climate Change Summary for Decision-Makers* (p. 5). United Nations Environment Programme. https://ledsgp.org/wp-content/uploads/2015/07/buildings-and-climate-change.pdf

86. Wang, M., & Gene, C. T. (1987). *Applied physics for architecture*. Tai Long book Co.

87. Wang, W., Zmeureanu, R., & Rivard, H. (2005). Applying multi-objective genetic algorithms in green building design Optimisation. *Building and Environment*, *40*(11), 1512–1525. https://doi.org/10.1016/j.buildenv.2004.11.017

88. Wang, X., Chen, D., & Ren, Z. (2010). Assessment of climate change impact on residential building heating and cooling energy requirement in Australia. *Building and Environment*, *45*(7), 1663–1682. https://doi.org/10.1016/j.buildenv.2010.01.022

89. York, R., Rosa, E. A., & Dietz, T. (2003). STIRPAT, IPAT and ImPACT: Analytic tools for unpacking the driving forces of environmental impacts. *Ecological Economics*, *46*(3), 351–365. https://doi.org/10.1016/S0921-8009(03)00188-5

90. Zain-Ahmed, A., Sopian, K., Othman, M. Y. H., Sayigh, A. A. M., & Surendran, P. N. (2002). Daylighting as a passive solar design strategy in tropical buildings: A case study of Malaysia. *Energy Conversion and Management*, *43*(13), 1725–1736. https://doi.org/10.1016/S0196-8904(01)00007-3